GKSS
FORSCHUNGSZENTRUM
in der HELMHOLTZ-GEMEINSCHAFT

Final Draft
of the original manuscript:

Atrens, A.; Winzer, N.; Dietzel, W.:
Stress Corrosion Cracking of Magnesium Alloys
In: Advanced Engineering Materials (2010) Wiley

DOI: 10.1002/adem.200900287

Overview of Stress Corrosion Cracking of Magnesium Alloys

Professor Dr. Andrej Atrens[1], Dr. Nicholas Winzer[2], Dr. Wolfgang Dietzel[3]
[1]The University of Queensland, Materials Engineering, Brisbane, Australia, 4072
[2]Fraunhofer Institute for Mechanics of Materials IWM, Freiburg, Germany
[3]GKSS-Forschungszentrum Geesthacht GmbH, Germany

Abstract
An overview is provided of our current understanding of SCC of Mg alloys. TGSCC is caused by an interaction of H with the microstructure so a detailed study of H-trap interactions is needed in order to design alloys resistant to TGSCC. This understanding is urgently needed because prior research indicates that many Mg alloys have a threshold stress for stress corrosion cracking of the order of half the yield stress in common environments including high-purity water.

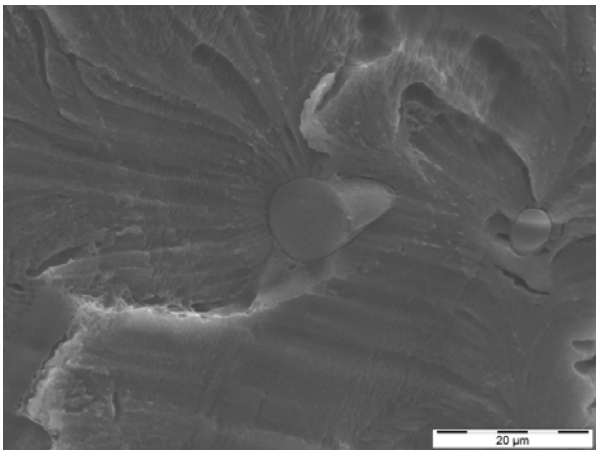

SCC fracture surface for AZ91 showing fracture of a β-particle ahead of the min crack

Introduction

This overview of stress corrosion cracking (SCC) of magnesium (Mg) alloys builds on our critical reviews of Mg corrosion [1-4] and Mg SCC [5]; and recent research to understand Mg corrosion [6-21] and SCC.[5,22-32] Our critical review of Mg SCC [5] found little published on SCC of cast Mg alloys, particularly modern alloys. This is in contrast to the considerable research on wrought Mg alloys during the 60s, 70s and 80s and on rapidly solidified Mg alloys in the early 90s, which was prompted by the aerospace and defence industries. Early reviews in 1966 reported that alloying addition such as Al and Zn to wrought Mg alloys promoted SCC; thus wrought AZxx alloys are susceptible to SCC for intermittent exposure to 0.01% NaCl and to the weather (i.e. humid air with intermittent

wetting and drying), whereas M1 and (the then existing) Zr containing alloys were reported to be free of SCC. Subsequent studies, summarised in our critical review [5], have mostly concentrated on pure Mg or Mg-Al alloys, but SCC has been shown for a number of Al-free alloys as summarised in Table 1.

Table 1. Values of SCC threshold stress, σ_{SCC}, for common Mg Alloys.[5]

Alloy, Environment	σ_{SCC}
HP Mg, 0.5%KHF_2	60%YS
Mg2Mn, 0.5%KHF_2	50%YS
MgMnCe, air, 0.001N NaCl, 0.01Na_2SO_4	85%YS
ZK60A-T5, rural atmosphere	50%YS
QE22, rural atmosphere	70-80%YS
HK31, rural atmosphere	70-80%YS
HM21, rural atmosphere	70-80%YS
HP AM60, distilled water	40-50%YS
HP AS41, distilled water	40-50%YS
AZ31, rural atmosphere	40%YS
AZ61, costal atmosphere	50%YS
AZ63-T6, rural atmosphere	60%YS
HP AZ91, distilled water	40-50%YS

SCC is a significant issue in Mg alloys. SCC can occur at stresses equal to 50% of the yield stress for many combinations of alloy + environment. This is in contrast to the earlier reports and to the perception of SCC resistance of pure Mg and Mg-Mn alloys. Clearly the early work needs to be checked, particularly for modern cast alloys. Since it is apparent that all Mg alloys are likely to be more or less susceptible, guidelines are needed to ensure safe application of Mg alloys in service. An urgent task is to delineate safe operational limits for common alloys in likely service environments. A way forward is to measure the threshold stress and threshold stress intensity factor for common commercial alloys in common service environments as enunciated in [5]. Table 1 indicates that it is conservative to assume that the threshold stress is ~40%YS, unless there is convincing data showing otherwise for the combination of Mg alloy and environment which is of specific interest.

SCC of Mg-Al alloys

Figures 1-3 [24-26] show stress versus apparent strain curves for AZ91, AZ31 and AM30, in distilled water and laboratory air, under CERT (constant extension rate test) conditions. AZ91 was machined from as-cast ingots, whereas AZ31 and AM30 were machined from large extrusions such that their tensile axis was parallel with the extrusion direction. The grain sizes were 50-100 m for AZ91 and 1-2 m for AZ31 and AM30 (equiaxed in all cases). AZ91 is a two-phase alloy containing significant amounts of the β-phase, $Mg_{17}Al_{12}$. AZ31 is largely a single α-phase alloy with a composition similar the α-phase of AZ91. AM30 is also single phase with a similar Al content as AZ31 but with Mn substituted for Zn. For specimens in distilled water, the apparent plastic deformation is largely attributed to SCC, with some contribution by the inert fracture mode, particularly at higher strain rates. In laboratory air, AZ91 had a lower σ_Y, higher strain hardening rate and lower ductility relative to AZ31 and AM30. The lower σ_Y is attributed to the larger grain size for

AZ91, whereas the lower ductility is largely attributed to the β-phase. The higher strain-hardening rate may be attributable to both the larger grain size and the presence of β-particles. In distilled water, all alloys suffered a reduction in UTS and apparent ductility relative to tests in laboratory air, with the UTS and apparent ductility decreasing with decreasing strain rate. The apparent ductility of AZ31 was considerably more sensitive to changes in strain rate than that of AZ91 and AM30.

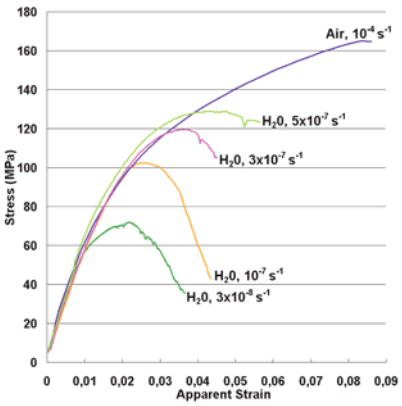

Figure 1. Stress vs apparent strain curves for AZ91.

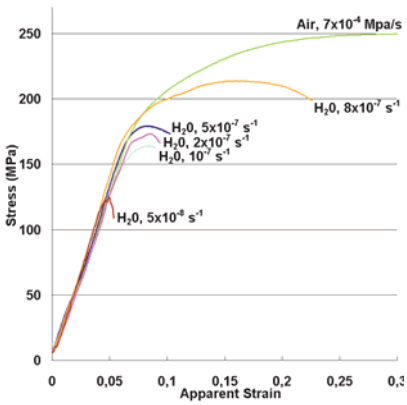

Figure 2. Stress vs apparent strain curves for AZ31.

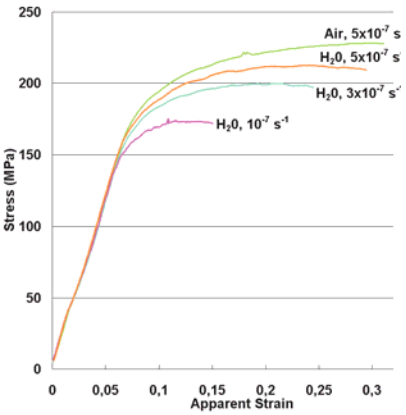

Figure 3. Stress vs apparent strain curves for AM30.

The SCC parameters, threshold stress, σ_{SCC} and stress corrosion crack velocity, V_c, for each strain rate ($\delta\varepsilon/\delta t$) are summarised in Table 2.[24-26] σ_{SCC} for AZ91 was significantly lower than for AZ31 and AM30 in magnitude, whereas AZ31 showed a higher relative susceptibility in terms of a lower value of σ_{SCC}/σ_Y at the lowest applied strain rate. There was a decrease in σ_{SCC} with decreasing strain rate for AZ91 and AZ31 (see also Figure 2 for AZ31); however, this trend was not identified for AM30 due to the narrower range of strain rates. There was an increase in V_c with increasing strain rate for AZ91. In contrast, V_c appeared independent of strain rate for AZ31 and AM30. V_c was considerably lower for AM30 than for AZ91 and AZ31, whilst V_c for AZ31 was slightly lower than for AZ91.

β-phase particles play an important role in SCC of AZ91, as evidenced by the nucleation of stress corrosion cracks within β-particles ahead of the crack tip, Figures 4 and 5. Crack nucleation within β-particles is probably due to (i) a reduction in their fracture toughness by trapped hydrogen; or (ii) the synergistic effects of hydrogen enhanced dislocation mobility and dislocation pile-ups at the α-β interface. The role of β-particles implies that the increasing SCC susceptibility of Mg alloys with increasing Al concentration is related to the distribution of, and propensity for crack nucleation within, β-particles. The increased susceptibility to SCC probably applies to all Mg alloys with large second phase particles.

Table 2. Threshold stress, σ_{SCC}, and SCC velocity, V_c, in distilled water.[24-26]

		AZ91 (σ_Y=70MPa, UTS=165MPa)				AZ31 (σ_Y=180MPa, UTS=250MPa)					AM30 (σ_Y=175MPa, UTS=230 MPa)		
$\delta\varepsilon/\delta t$	$x10^{-8}$ s^{-1}	3	10	30	50	5	10	20	50	80	10	30	50
σ_{SCC}	MPa	55	60	75	70	105	145	165	160	170	140	130	140
σ_{SCC}/σ_Y		0.79	0.87	1.1	1.0	0.58	0.81	0.92	0.89	0.94	0.80	0.74	0.80
V_c	$x10^{-9}$ m/s	1.6	3.7	11	12	4.4	2.0	6.7	1.2	5.5	0.36	0.93	0.55

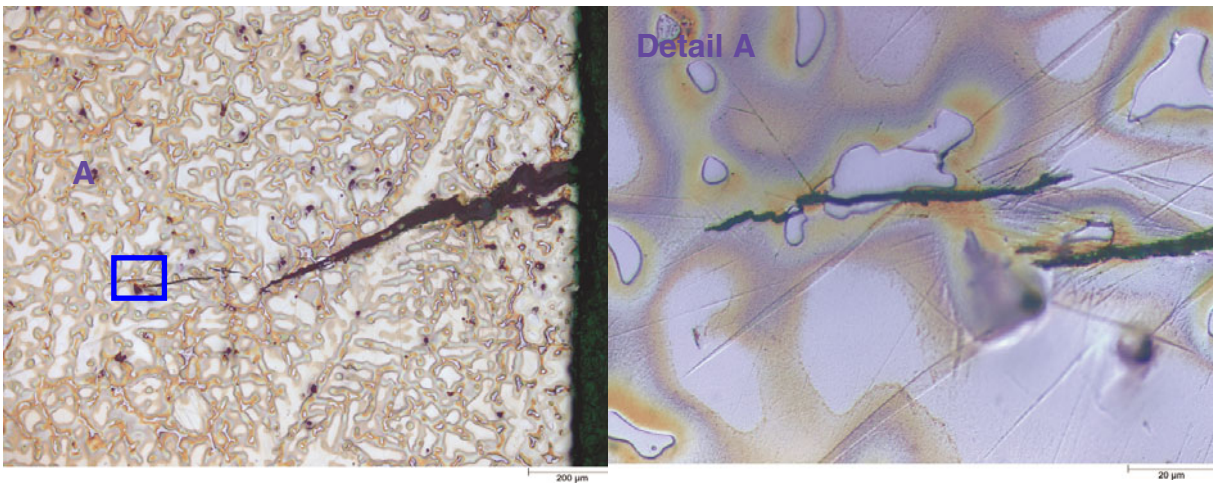

Figure 4. Secondary crack in AZ91.

The fracture surfaces for AZ91 specimens tested in distilled water at very slow strain rates, Figure 6, were similar to those resulting from pre-charging in gaseous H_2 to induce hydride precipitation, implying that the quantity of H transported ahead of the crack tip during SCC of AZ91 at very slow crack velocities is sufficient for substantial hydride precipitation. It indicates that there is an urgent requirement for a better understanding of the H diffusivity and solubility in Mg alloys [33] at temperatures relevant to SCC.

In contrast to the increasing SCC susceptibility with decreasing strain rate in distilled water as shown in Fig.s 1-3, Ebtehaj et al [34] found maximum susceptibility in NaCl + K_2CrO_4 solutions at intermediate strain rates. The influence of strain rate was ascribed to, at low strain rates, the balance between repassivation and mechanical film rupture at the crack tip and, at high strain rates, the propensity for the inert fracture mechanism to overwhelm the SCC fracture mechanism. In contrast for SCC in distilled water, Fig.s 1-3, decreasing strain rate caused a continuous increase in SCC susceptibility, characterised by: (i) an increasing difference between σ_{SCC} and the UTS; (ii) a decreasing elongation-to-failure; and (iii) a decrease in σ_{SCC} for AZ91 and AZ31. In distilled water, the influence of repassivation at the crack tip is negligible, and the influence of strain rate is related to the mechanism for crack propagation. In contrast, Ebtehaj et al [34] used strongly passivating solutions. This indicates that the occurrence of maximum SCC susceptibility at intermediate strain rates for Mg alloys in strongly passivating solutions is a characteristic of these environments rather than a characteristic of Mg alloys.

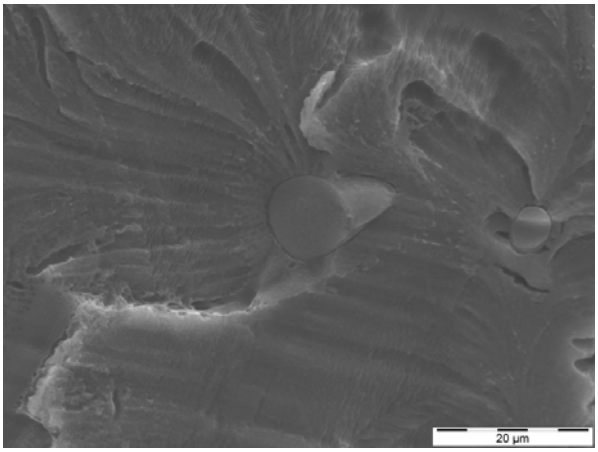

Figure 5. SCC fracture surface for AZ91 showing the influence of β-particles on the orientation of parallel markings.

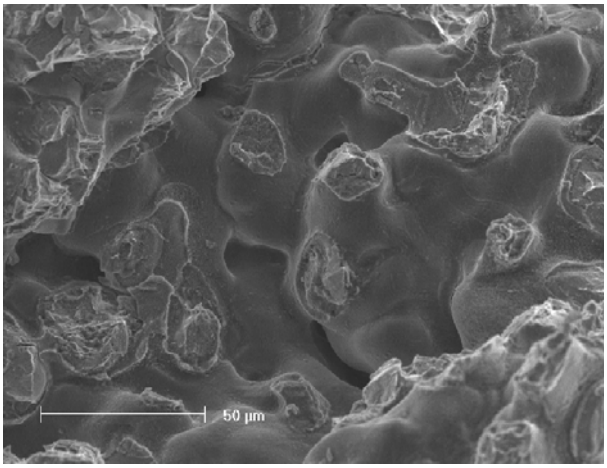

Figure 6. Fracture surface morphology for AZ91 in distilled water at $3x10^{-8}$ s^{-1} showing quasi-porous features.

The mechanism for SCC initiation in AZ31 and AM30 is different in CERT and LIST, Lineraly Increasing Stress Test [35], whereas the propagation mechanism is the same. Moreover the initiation and propagation mechanism is the same in LIST. In CERT, SCC initiation involves transgranular localised dissolution, possibly due to mechanical film rupture at emerging slip steps. For AZ31 and AM30, in CERT, the mechanism for crack growth changes from localised dissolution to HE at some critical crack length. There were differences in the mechanisms or rate limiting processes for HE in AZ31 and AM30, manifested in: (i) V_c; (ii) the crystallography of cleavage-like fracture surface markings; and (iii) the appearance of micro-dimples within the cleavage-like facets. These differences may be attributed to the influences of Zn and second phase particles (more concentrated in AZ31) on H diffusivity in the α-matrix. The influences of Zn and second phase particles could be such that: (i) different HE mechanisms occur for AZ31 and AM30; or (ii) the same HE mechanism occurs in AZ31 and AM30, with the difference in H diffusivity affecting V_c and the fracture surface morphology.

Medical applications

There is growing interest for Mg as a degradable medical implant.[36-40] Kannan and Raman [41] found small decreases of strength and ductility for AZ91 in a simulated body fluid using CERT; these decreases usually indicate SCC although the decreases were claimed to be insignificant.

LIST vs CERT

The LIST apparatus [35] is illustrated in Figure 7. The specimen is attached to one end of a lever arm. On the opposite end of the arm a known mass is lowly moved outwards such that the tensile load applied to the specimen increases linearly as the distance between the fulcrum and the mass is increased by means of a screw thread and synchronous motor.

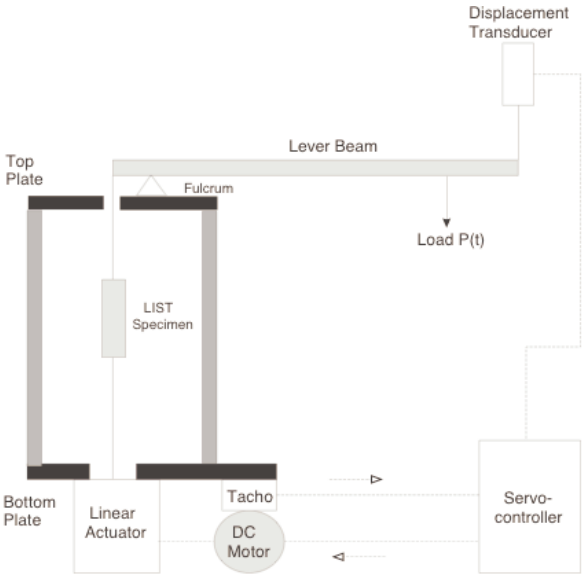

Figure 7. Schematic of the LIST apparatus. LIST can be considered as load controlled CERT.

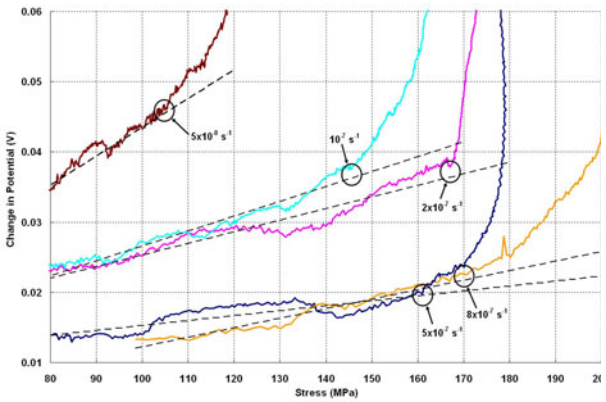

Figure 8. Specimen resistance versus stress for AZ31 in distilled water, during CERT, and estimation of threshold stress.

Transgranular stress corrosion cracking (TGSCC) of the Mg alloy AZ91 in distilled water and 5 g/L NaCl solution was evaluated [24] using LIST and CERT. LIST and CERT both load the specimen until fracture; LIST is load controlled whereas CERT is displacement controlled. LIST and CERT are both useful in identifying the occurrence of SCC. The threshold stress can be identified in both techniques by using a potential drop technique to measure the change in specimen resistance during the test as illustrated in Figure 8. The tests are essentially identical until crack initiation. During a LIST, fast fracture ensues a relatively short time after the threshold stress is attained, when the stress corrosion crack reaches the critical crack size. In contrast, during CERT crack growth occurs over a much longer time period. Consequently, LIST is typically 30-50 % shorter in duration, whereas CERT produces a larger SCC fracture surface. However, the stress corrosion crack in CERT may be different particularly in the later stages when there can be a significant decrease in stress. In addition, the SCC initiation in AZ31 and AM30 was different in CERT and LIST as summarized above.

Delayed Hydride Cracking Mechanism

Winzer et al [22] evaluated the delayed hydride cracking (DHC) mechanism for transgranular stress corrosion cracking (TGSCC) of Mg alloys as this was a likely SCC mechanism based on prior understanding [5]. A DHC model was formulated with the following components: (i) transient H diffusion towards the crack tip driven by stress and H concentration gradients; (ii) hydride precipitation as the H solvus is exceeded; and (iii) crack propagation through the hydride when it reaches a critical size of ~0.8 m (the distance between crack arrest markings from [42]). The stress corrosion crack velocity, V_c, was calculated from the time, t, for the hydride to reach the critical size as $V_c = (0.8 \text{ m})/t$. The model was implemented using a finite element script developed in MATLAB. The input parameters were chosen, based on the information available, to determine the highest

possible value for V_c. Values for V_c of ~10^{-7} m/s were predicted by this DHC model. These predictions are consistent with measured values for V_c for Mg alloys in distilled water, including those in Table 2, but cannot explain values for V_c of ~10^{-4} m/s measured in other aqueous environments. Insights for understanding Mg TGSCC were drawn. A key outcome is that the assumed initial condition for the DHC models is unlikely to be correct. During steady state stress corrosion crack propagation of Mg in aqueous solutions, a high dynamic hydrogen concentration would be expected to build up immediately behind the crack tip. Stress corrosion crack velocities ~ 10^{-4} m/s, typical for some Mg alloys in some aqueous solutions, might be predicted using a DHC model for Mg based on the time to reach a critical hydride size in steady state, with a significant residual hydrogen concentration from the previous crack advance step.

Welding

Welding is often used to fabricate engineering structures. The microstructure is typically changed due to the thermal cycle and the weld metal can have a composition different to the parent metal. These changes in microstructure and chemical composition may influence SCC. There is extensive research on Mg welding.[43-47] Laser butt (LB) welding has the following advantages: (i) high welding speed; (ii) very narrow joints with a reduced heat affected zone (HAZ) and low distortion; and (iii) a high joint efficiency (joint strength/base metal strength) approaching 100% [43], whereas conventional fusion welding, such as tungsten inert gas (TIG) welds, have joint efficiencies of ~70–90%.[44] Friction stir welding (FSW)[46] achieves a metallic bond at temperatures below the melting point thereby avoiding issues associated with alloy melting.[47]

A few researchers [48-50] have studied SCC of welded Mg. Winzer et al [50] found high SCC susceptibility of TIG welds of continuous-cast AZ31. SCC initiated at the interface between the weld metal and the HAZ. Kannan et al. [48] reported high SCC susceptibility of LB-welded AZ31. SCC occurred in the fusion boundary. SCC was caused by galvanic corrosion between the fusion zone and the base metal, attributed to the difference in Al concentration. The fracture was mixed IGSCC and TGSCC. The SCC susceptibility for fusion welded Mg alloys appears to be caused by the ease of producing significant galvanic corrosion. Kannan et al. [49] also reported SCC in FSW AZ31; SCC occurred in the stir zone (SZ) and the SCC was attributed to hydrogen assisted cracking. Bala et al. [51,52] found SCC for plasma electrolytic oxidation (PEO) coated LB welded AZ31 and FSW AZ61. The PEO coating provided protection against corrosion but not against SCC.

Influence of RE

Mg alloys incorporate rare-earth (RE) elements [53] to improve (i) creep resistance, which is primarily achieved by RE-containing phases along grain boundaries [54,55], (ii) castability, (iii) age hardening [56], and (iv) corrosion resistance [57]. Chang et al. [57] reported that Mg-3Nd-0.2Zn-0.4Zr had a corrosion rate lower than AZ91D. Nordlien et al.[58] reported that RE elements improved passivation. Krishnamurthy et al.[59] suggested that pseudo-passivation in rapidly solidified Mg-Nd is due to Nd enrichment at the surface.

The literature on SCC of RE containing Mg alloys is limited.[5,23,53] The summary of data in Winzer et al. [5] indicated that Nd had little or no influence on SCC susceptibility, whereas Rokhlin [53] reported that Nd addition to Mg-Zn-Zr increased SCC resistance. Kannan et al. [23] found SCC for three RE alloys (ZE41, QE22 and EV31A) and AZ80 in 0.5 wt.% NaCl and in distilled water. TGSCC in AZ80, ZE41 and QE22 in distilled water and in AZ80 in 0.5 wt.% NaCl was consistent with HE, whereas IGSCC in ZE41, QE22 and EV31A in 0.5 wt.% NaCl was caused by micro-galvanic corrosion associated with the second phase along grain boundaries, Fig. 9.

Significance and Future Directions

SCC can occur in any application when a stressed Mg-based component is subject to wet conditions. Catastrophic failure is expected when hydrogen, introduced into the Mg from the Mg corrosion reaction, decreases the SCC initiation stress to below the operating stress. The risk is increased by high operating stresses, which can exceed the yield stress.

Intergranular stress corrosion cracking (IGSCC) of Mg alloys is reasonably well understood. IGSCC in Mg alloys, illustrated in Figure 9 for EV31A [23], occurs typically by micro-galvanic corrosion caused if there is a continuous second phase along the grain boundaries, a microstructure typical of many creep-resistant Mg alloys. In contrast, transgranular stress corrosion cracking (TGSCC), illustrated in Figure 10, occurs through the α-phase Mg matrix. TGSCC is the intrinsic form of SCC and can occur in alloys resistant to IGSCC. TGSCC occurs for common Mg alloys in environments such as distilled water and dilute chloride solutions as summarized above. The potential impact of TGSCC is indicated by the fact that the initiation stress may be as low as half the yield stress.

Mg alloys are starting to be used in structural applications and new classes of wrought Mg alloys are emerging. These include high-performance high-strength heat-treatable wrought alloys. Promising alloy systems include Mg-Zn-Φ, Mg-Sn-Λ and Mg-RE-Σ. Their SCC behaviour has not been characterized. Clearly, significant risk of SCC would negate much of the potential for application of Mg alloys in critical service components, such as stents (catastrophic fracture due to SCC in a heart artery would probably be fatal) or stressed Mg-alloy auto components that are exposed to road spray, including body sheet.

Mg TGSCC involves repeated cycles of (i) H diffusion to the stressed region ahead of the crack tip and (ii) stress corrosion crack advance through the H-influenced zone of size ~1 m. H is produced as part of the Mg corrosion reaction, which occurs at breaks in the partially protective surface film; the breaks in the surface film are caused by the environment and loading. Our recent research [24-27] has shown that TGSCC for different Mg alloys occurs by different H mechanisms. SCC in AZ91 is initiated by H facilitated fracture of β-phase particles and propagates by HELP (H enhanced localised plasticity) through the α-phase. HELP is also the SCC propagation mechanism through the α-phase in AZ31 whereas SCC propagation through the α-phase in AM30 is by HEDE (H enhanced decohesion). The TGSCC initiation stress for AZ31 and AM30 is significantly higher than for AZ91, indicating that the initiation stress is dependent of the Mg

microstructure, and furthermore indicating that Mg alloy improvements can be expected from understanding the influences of microstructure.

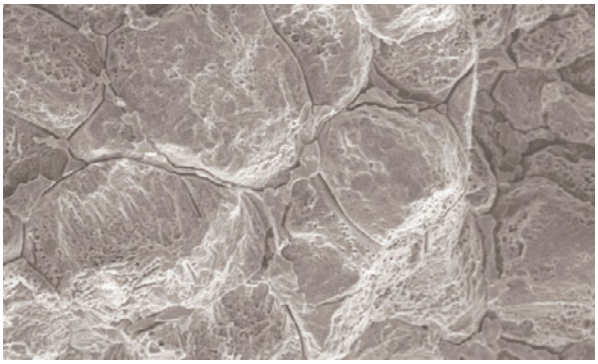

Figure 9. SCC of EV31A in 5g/L NaCl. CERT.[23]

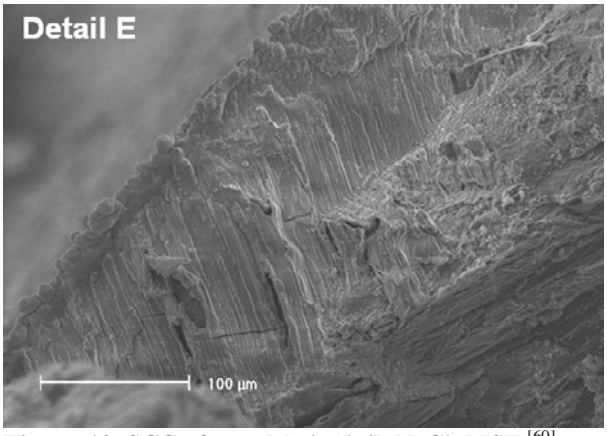

Figure 10. SCC of pure Mg in 5g/L NaCl. LIST.[60]

All two-phase alloys, like AZ91, are expected to have poor TGSCC properties if there is H-facilitated fracture of the large second-phase particles. In contrast, at present there is no information regarding the H-influenced fracture behaviour of the small precipitates that are effective for precipitation hardening, although there are promising indications, extrapolating from their positive influence for some heat treatment conditions in Al alloys. SCC resistance is much higher for Al alloys in the over-aged condition and for particular double aging conditions [61].

AM30 has a SCC propagation velocity significantly lower than that of AZ31 and AZ91 [24-27], consistent with a lower effective H diffusivity, probably due to the absence of Zn in AM30. This again demonstrates the necessity to understand the influence of solid-solution alloying on SCC propagation velocity and H diffusivity.

The next major advance in understanding Mg TGSCC requires an understanding of the microstructure influences on SCC. Included needs to be an understanding of the effective H diffusion rate to the fracture process zone. This requires an understanding of H-trap interactions in Mg alloys.

Acknowledgements

The authors wish to thank the GM Technical Centre at Warren MI, the Australian Research Council (ARC), the Australian Research Network for Advanced Materials (ARNAM) and GKSS-Forschungszentrum Geesthacht GmbH.

References

1 G. Song, A. Atrens, *Adv. Eng. Mater.* **1999**, *1*, 11.
2 G. Song, A. Atrens, *Adv. Eng. Mater.* **2003**, *5*, 837.

3 G. Song, A. Atrens, *Adv. Eng. Mater.* **2007**, *9*, 177.
4 Z Shi, M Liu, A Atrens, *Corrosion Science*, 10.1016/j.corsci.2009.10.016
5 N. Winzer, A. Atrens, G. Song, E. Ghali, W. Dietzel, K.U. Kainer, N. Hort, C. Blawert, *Adv. Eng. Mater.* **2005**, *7*, 659.
6 MC Zhao, P Schmutz, S Brunner, M Liu, G Song, A Atrens, *Corrosion Science*, **2009**, *51*, 1277.
7 A Seyeux, M Liu, P Schmutz, G Song, A Atrens, P Marcus, *Corrosion Science*, **2009**, *51*, 1883
8 M Liu, P Schmutz, S Zanna, A Seyeux, H Ardelean, G Song, A Atrens, P Marcus, *Corrosion Science*, 10.1016/j.corsci.2009.10.015
9 M.C. Zhao, M. Liu, G. Song, A. Atrens, *Corros. Sci.* **2008**, *50*, 1939.
10 M.C. Zhao, M. Liu, G. Song, A. Atrens, *Corros. Sci.* **2008**, *50*, 3168.
11 M.C. Zhao, P. Schmutz, S. Brunner, M. Liu, G. Song, *Corros. Sci.* **2009**, *51*, 1277.
12 MC Zhao, M Liu, G Song, A Atrens, *Advanced Engineering Materials*, **2008**, *10*, 93.
13 M.C. Zhao, M. Liu, G. Song, A. Atrens, *Adv. Eng. Mater.* **2008**,*10*, 104.
14 M. Liu, P. J. Uggowitzer, A.V. Nagasekhar, P. Schmutz, M. Easton, G. Song, A. Atrens, *Corros. Sci.* **2009**, *51*, 602.
15 M Liu, S Zanna, H Ardelean, I Frateur, P Schmutz, G Song, A Atrens, P Marcus, *Corros. Sci.* **2009**, *51*, 1115.
16 JX Jia, GL Song, A Atrens, *Corrosion Science*, **2006**, *48*, 2133.
17 A Atrens, W Dietzel, *Advanced Engineering Materials*, **2007**, *9*, 292.
18 S Bender, J Goellner, A Atrens, *Advanced Engineering Materials*, **2008**, *10*, 583.
19 W.C. Neil, M. Forsyth, P.C. Howlett, C.R. Hutchinson, B.R.W. Hinton, *Corrosion Science* **2009**, *51*, 387.
20 J Chen, J Dong, J Wang, E Han, W Kev, *Corrosion Science,* **2008**, *50*, 3610.
21 N. Birbilis, M.A. Easton, A.D. Sudholz, S.M. Zhu, M.A. *Corrosion Science*, **2009**, *51*, 683
22 N Winzer, A Atrens, W Dietzel, G Song, KU Kainer, *Mater. Sci. Eng. A,* **2007**, *466*, 18.
23 MB Kannan, W Dietzel, C Blawert, A Atrens, P Lyon, *Mater. Sci. Eng A*, **2008**, *480*, 529.
24 N Winzer, A Atrens, W Dietzel, G Song, KU Kainer, *Mater. Sci. Eng. A*, **2008**, *472* 97.
25 N Winzer, A Atrens, W Dietzel, VS Raja, G Song, KU Kainer, *Mater. Sci. Eng. A*, **2008**, *488*, 339.
26 N Winzer, A Atrens, W Dietzel, G Song, KU Kainer, *Metall. Mater. Trans. A*, **2008**, *39*, 1157.
27 N Winzer, A Atrens, W Dietzel, G Song, KU Kainer, *Adv. Eng. Mater.*, **2008**, *10*, 453.
28 J Chen, J Wang, E Han, J Dong, W Ke *Corrosion Science*, **2008**, *50*, 1292
29 Arnon, E. Aghion, *Advanced Engineering Materials*, **2008**, *10*, 742.
30 J. Chen, M, Ai, J. Wang, E. Han, W. Ke, *Materials Science and Engineering A*, **2009**, *515*, 79.
31 M.B. Haroush, C.B. Hamu, D. Eliezer, L. Wagner, *Corrosion Science*, **2008**, *50*, 1766.
32 J Chen, J Wang, E Han, W Ke, *Materials Science and Engineering A*, **2008**, *488*, 428.
33 A Atrens, N Winzer, GL Song, W Dietzel, C Blawert, *Adv. Eng. Mater.*, **2006**, *8*, 749.

34 K. Ebtehaj, D. Hardie, R.N. Parkins, *Corrosion Science,* **1993,** *28,* 811
35 A Atrens, CC Brosnan, S Ramamurthy, A Oehlert, IO Smith, Measurement Sci. and Technol. **1993**, *4*, 1281.
36 F Witte, J Fischer, F Bechman, M Stoemer, N Hort, *Scripta Materialia*, **2008**, *58*, 453.
37 F Witte, F Feyerabend, P Maier, J Fischer, M Stromer, C Blawert, W Dietzel, N Hort, *Biomaterials*, **2007**, *28*, 2163.
38 F Witte, H Ulrich, M Rudert M, E Wildbold, *Journal Of Biomedical Materials Research Part A*, **2007**, *81A*, 748.
39 F Witte F, H Ulrich, C Palm, E wildbold, *Journal Of Biomedical Materials Research Part A*, **2007**, *81A*, 757.
40 B. Zberg, P. J. Uggowitzer, J. F. Loffler, *Nature Materials,* 2009, *8*, 887.
41 M.B. Kannan, R.K.S. Raman, Biomaterials, **2008**, *29*, 2306.
42 DG Chakrapani, EN Pugh, *Metall. Trans. A*, **1976**, *7*, 173,
43 A. Munitz, C. Cotler, H. Shaham, G. Kohn, *Weld. J.*, **2000**, *7*, 202.
44 J. Matsumoto, M. Kobayashi, M. Hotta, *Weld. Int.*, **1990**, *4*, 23.
45 X. Cao, M. Jahazi, J.P. Immarigeon,W.Wallace, *J. Mater. Process. Technol.*, **2006**, *171*, 188.
46 W.M. Thomas, *U.S. Patent No.* 5,460,317
47 R. Zettler, A.C. Blanco, J.F. dos Santos, S. Marya, in: N.R. Neelameggham, H.I. Daplan, B.R. Powell (Eds.), *Magnesium Technology*, TMS, The Minerals, Metals & Materials Society, **2005**
48 M.B. Kannan, W. Dietzel, C. Blawert, S. Riekehr, M. Kocak, *Materials Science and Engineering A*, **2007**, *444*, 220.
49 M.B. Kannan, W. Dietzel, R. Zeng, R. Zettler, J.F. dos Santos, *Materials Science and Engineering A*, **2007**, *460-461*, 243.
50 N. Winzer, P.Xu, S.Bender, T.Gross, W.E.S. Unger, C.E.Cross, *Corrosion Science*, (2009), doi:10.1016/j.corsci.2009.05.037
51 P. Bala Srinivasan, R. Zettler, C. Blawert, W. Dietzel, *Materials Characterization*, **2009**, *60*, 389.
52 P.B. Srinivasan, S. Riekehr, C. Blawert, W. Dietzel, M. Kocak, *Materials Science and Engineering A*, **2009**, *517*, 197.
53 L.L. Rokhlin, *Magnesium Alloys Containing Rare Earth Metals*, Taylor and Francis, London, **2003**
54 J.F. Nie, X. Gao, S.M. Zhu, *Scr. Mater.*, **2005**, *53*, 1049.
55 C. Sanchez, C. Nussbaum, P. Azavant, H. Octor, *Mater. Sci. Eng. A*, **1996**, *221*, 48.
56 P. Lyon, T.Wilks, I. Syed, in: N.R. Neelameggham, H.I. Kaplan, B.R. Powell (Eds.), *Magnesium Technology 2005*, Warrendale, PA, **2005**, 303
57 J. Chang, X. Guo, P. Fu, L. Peng, W. Ding, *Electrochim. Acta*, **2007**, *52*, 1360.
58 J.H. Nordlien, K. Nisancioglu, S. Ono, N. Masuko, *J. Electrochem. Soc.*, **1997**, *144*, 461.
59 S. Krishnamurthy, M. Khobaib, E. Robertson, F.H. Froes, Mater. Sci. Eng. A, **1988**, *99*, 507.
60 N Winzer, G Song, A Atrens, W Dietzel, C Blawert, *Corros. Preven. 2005*, ACA, **2005**, 37.
61 RG Song, W Dietzel, BJ Zhang, WJ Liu, M Tseng, A Atrens, *Acta Mater.*, **2004**, *52*, 4727.